Key Points:

- Radiative cooling by volcanic aerosol over the tropical northern Africa triggers El Niño-like conditions via atmospheric circulation changes
- The "ocean thermostat mechanism" is absent in our simulations when a uniform aerosol forcing is applied over the equatorial Pacific (EqPAC)
- The Maritime Continent cooling mechanism is not at play when the aerosol forcing extends over the entire EqPAC

Author Contributions:

Conceptualization: Francesco S. R. Pausata
Formal analysis: Francesco S. R. Pausata, Yang Zhao, Davide Zanchettin
Methodology: Francesco S. R. Pausata
Writing – original draft: Francesco S. R. Pausata
Writing – review & editing: Yang Zhao, Davide Zanchettin, Rodrigo Caballero, David S. Battisti

Revisiting the Mechanisms of ENSO Response to Tropical Volcanic Eruptions

Francesco S. R. Pausata[1] [ID]**, Yang Zhao[2]** [ID]**, Davide Zanchettin[3]** [ID]**, Rodrigo Caballero[4]** [ID]**, and David S. Battisti[5,6]**

[1]Department of Earth and Atmospheric Sciences, Centre ESCER (Étude et la Simulation du Climat à l'Échelle Régionale) and GEOTOP (Research Center on the dynamics of the Earth System), University of Quebec in Montreal, Montreal, QC, Canada, [2]State Key Laboratory of Severe Weather, Chinese Academy of Meteorological Sciences, Beijing, China, [3]Department of Environmental Sciences, Informatics and Statistics, University Ca'Foscari of Venice, Mestre, Italy, [4]Department of Meteorology, Stockholm University and Bolin Centre for Climate Research, Stockholm, Sweden, [5]Department of Atmospheric Sciences, University of Washington, Seattle, WA, USA, [6]UNI Research, Bergen, Norway

Abstract Stratospheric volcanic aerosol can have major impacts on global climate. Despite a consensus among studies on an El Niño-like response in the first or second post-eruption year, the mechanisms that trigger a change in the state of El Niño-Southern Oscillation (ENSO) following volcanic eruptions are still debated. Here, we shed light on the processes that govern the ENSO response to tropical volcanic eruptions through a series of sensitivity experiments with an Earth System Model where a uniform stratospheric volcanic aerosol loading is imposed over different parts of the tropics. Three tropical mechanisms are tested: the "ocean dynamical thermostat" (ODT); the cooling of the Maritime Continent; and the cooling of tropical northern Africa (NAFR). We find that the NAFR mechanism plays the largest role, while the ODT mechanism is absent in our simulations as La Niña-like rather than El-Niño-like conditions develop following a uniform radiative forcing over the equatorial Pacific.

Plain Language Summary Volcanic eruptions emit large quantity of sulfate aerosol up to the stratosphere. Such aerosol can alter global climate by interacting with solar radiation and in turn modifying atmospheric and ocean circulation. In particular, volcanic aerosol can alter the state of the El Niño-Southern Oscillation (ENSO), the major mode of tropical climate variability. However, the mechanisms that trigger a change in the ENSO state following volcanic eruptions are still debated. In this study, we use an Earth System Model to revisit the main mechanisms that have been proposed to alter ENSO, causing positive temperature anomalies over the equatorial Pacific (EqPAC) Ocean. We tested three mechanisms: the "ocean dynamical thermostat" (ODT); the cooling of the Maritime Continent; and the cooling of tropical northern Africa (NAFR). Our experiments show that the NAFR mechanism plays the largest role, while the ODT mechanism is absent in our simulations as cold rather than warm develop over the EqPAC Ocean following the applied volcanic forcing.

1. Introduction

Large explosive volcanic eruptions can have major impacts on global climate, affecting both radiative balance and inducing interannual-to-decadal dynamical alterations of the atmospheric and ocean circulation (e.g., Timmreck, 2012; Zanchettin, 2017). Such impacts are mainly due to the injection of large quantities of sulfur dioxide into the stratosphere, which are oxidized and then converted into sulfate aerosols. Consequently, the stratospheric aerosol layer is enhanced for 2–3 years following major eruptions, during which the aerosol scatters some incoming solar radiation back to space cooling the surface (e.g., Timmreck, 2012).

The global average surface cooling reaches its maximum 6–18 months after the peak net direct radiative forcing corresponding to the maximum enhancement of the stratospheric volcanic aerosol layer (Thompson et al., 2009). Volcanic eruptions induce dynamical responses in the Earth system as well, which are seen as modulation of natural modes of climate variability, such as the Arctic Oscillation/North Atlantic Oscillation (Christiansen, 2008; Kodera, 1994; Shindell, 2004) and the El Niño-Southern Oscillation (ENSO) (Emile-Geay et al., 2008; McGregor & Timmermann, 2011). Given the profound influence of ENSO on global climate and its strong societal relevance, it is important to understand how volcanism can modulate ENSO. Such understanding may enhance predictability of subsequent El Niño/La Niña events following future volcanic eruptions.

Despite some discrepancies across studies regarding the response of ENSO to volcanic forcing based on paleoclimate reconstructions (e.g., Adams et al., 2003; Dee et al., 2020; Li et al., 2013), McGregor et al. (2020) showed that the majority of available reconstructions (12 out of 17 reconstructions) display an El Niño-like warming in the year of eruption, while none display a significant La Niña-like response when provided with consistent dates of volcanic eruptions. Furthermore, McGregor et al. (2020) identify an emerging consensus from the numerous coupled General Circulation Model (CGCM) studies investigating the impact of tropical volcanism on ENSO, with the overwhelming majority displaying an El Niño-like warming in the year following the eruption. However, different aerosol spatial distributions, hence differences in the spatial structure of volcanic forcing, may trigger different ENSO responses. Stevenson et al. (2016) investigated the impact of Northern Hemisphere (NH), Southern Hemisphere (SH) and tropical volcanic eruptions using the Community Earth System Model-Last Millennium Ensemble (CESM-LME). They concluded that while NH and tropical eruptions tend to favor El Niño-like conditions, SH eruptions enhance the probability of La Niña-like events within 1 year from the eruptions. Similar results were found by Pausata et al. (2020) and Ward et al. (2021) using different CGCMs (NorESM1-M and MPI-ESM, respectively). Conversely, Zuo et al. (2018), also using the CESM-LME, concluded that SH, NH and tropical eruptions all resulted in El Niño-like conditions in the year of the eruption—albeit weak for SH eruptions. However, Zuo et al. (2018) define ENSO anomalies relative to zonal mean cooling, introducing methodological specificities, particularly regarding the separation of dynamical ENSO responses from tropical radiative cooling, that may in part explain differences with previously published results.

The mechanisms that trigger changes in the ENSO state following volcanic eruptions are still debated. When an eruption results in an aerosol distribution with strong hemispheric asymmetry, the impact on the evolution of ENSO is robust across models and is mostly governed by energetic constraints (Kang et al., 2008; Schneider et al., 2014). The associated asymmetric cooling of the hemispheres features meridional shifts in the Intertropical Convergence Zone (ITCZ) (Atwood et al., 2020) and subsequent coupled atmosphere-ocean feedbacks in the tropical Pacific (Colose et al., 2016; Pausata, Chafik, et al., 2015; Pausata, Karamperidou, et al., 2016; Pausata et al., 2020; Stevenson et al., 2016). An eruption, yielding aerosol that is concentrated in the NH, moves the ITCZ in the Pacific equatorward, weakening the trade winds and leading to an El Niño-like anomaly via the Bjerknes feedback. In contrast, aerosol concentrated in the SH moves the ITCZ northward inducing a strengthening of the trade winds along the equator, hence triggering La Niña-like anomalies.

The mechanisms triggering the ENSO response to a tropical eruption that results in a weak hemispheric asymmetry are not hitherto fully understood, however. One of the most frequently adopted hypotheses is the "ocean dynamical thermostat" mechanism (ODT) (Clement et al., 1996), where a uniform negative radiative forcing over the equatorial Pacific (EqPAC) initially induces less cooling in the eastern relative to the western Pacific due to the presence of strong ocean upwelling in the eastern Pacific, which helps maintain the sea-surface temperature (SST) there close to the temperature of the upwelling water. The weakened zonal SST gradient along the EqPAC causes a relaxation of the trade winds and reduces the ocean upwelling in the eastern Pacific. This process is then amplified by the Bjerknes feedback, resulting in an El Niño response to volcanic forcing (Bjerknes, 1969). The ODT mechanism emerged in simulations with an idealized model (the Zebiak-Cane model (Zebiak & Cane, 1987)) and an imposed uniform radiative cooling (Clement et al., 1996; Emile-Geay et al., 2008; Hirono, 1988; Mann et al., 2005). However, recent studies have questioned the existence of the ODT mechanism in CGCMs (e.g., Pausata et al., 2020; Stevenson et al., 2016; Ward et al., 2021).

Another suggested mechanism for the ENSO response to a tropical aerosol forcing is based on the land-ocean temperature gradient (Ohba et al., 2013; Predybaylo et al., 2017), which is enhanced after a volcanic eruption as land areas (e.g., the Maritime Continent (MC) (Ohba et al., 2013) or Southeast Asia (Predybaylo et al., 2017)) initially cools faster than the ocean. The increased land-ocean temperature gradient would then initiate a westerly wind anomaly in the western EqPAC, leading to an El Niño-like anomaly through the Bjerknes feedback.

Finally, Khodri et al. (2017) proposed a mechanism whereby atmospheric teleconnections are the source of an altered Walker circulation in post-eruption years. According to this mechanism, the reduction of the tropical precipitation over Africa and tropospheric cooling causes anomalous atmospheric Kelvin waves in boreal fall that weaken the trade winds over the western Pacific, leading to El Niño-like conditions in the year after a major eruption. However, there is no consensus yet as to which of these proposed mechanisms is the main driver of the ENSO response after large tropical volcanic eruptions.
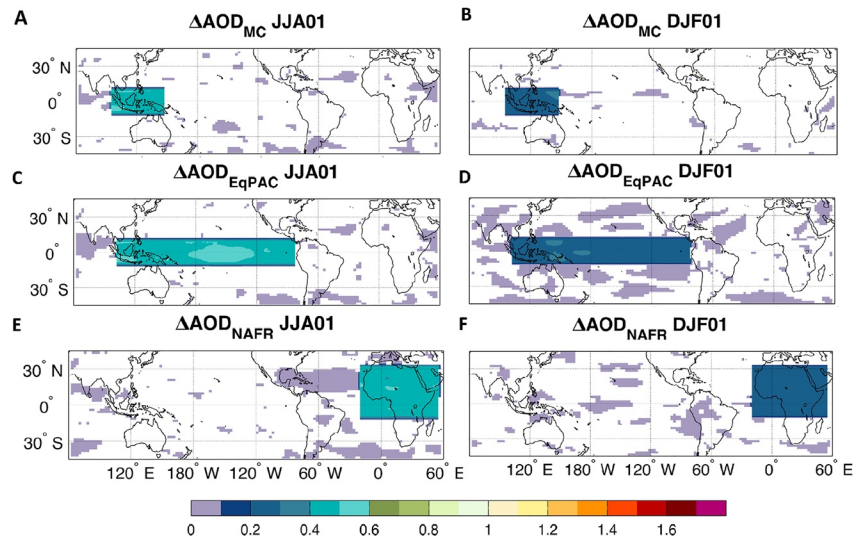
Figure 1. Volcanic forcing. Anomalies in aerosol optical depth (AOD) relative to the no volcano experiment NV. Forcing is localized to the (top) Maritime Continent (MC), (middle) the equatorial Pacific (EqPAC), and (middle) tropical and northern Africa (NAFR) (bottom). The forcing is applied on 1 June, and anomalies are shown for the summer (June to August, JJA; left) and winter (December to February, DJF; right) following the imposed changes in AOD.

Here, we design and perform a series of sensitivity experiments to isolate each of the three tropical mechanisms that have been brought forward for the ENSO response to tropical volcanic eruptions. Specifically, we perform "volcano" experiments in which we impose a uniform spatially fixed aerosol loading over different parts of the tropics (Figure 1) starting in June and lasting for about 1.5 years (Figure S1 in Supporting Information S1). These experiments are meant to shed light on the processes that govern the ENSO response as a function of the regional distribution of the aerosol forcing.

2. Model Description and Experimental Setup

2.1. Model Description

We used the Norwegian Earth System Model (NorESM1-M (Bentsen et al., 2013; Iversen et al., 2013)) to simulate a set of sensitivity experiment in which we prescribe aerosol concentrations over specific areas of the tropics to test the above-mention mechanisms that could potentially trigger the post-volcano ENSO response. NorESM1-M has a horizontal resolution of $1.9°$ (latitude) $\times 2.5°$ (longitude) and 26 vertical levels and uses a modified version of Community Atmospheric Model version 4 (CAM4 (Neale et al., 2013)), CAM4-Oslo, to simulate the atmospheric circulation with an updated module that simulates the life cycle of aerosol particles, and primary and secondary organics. NorESM1-M includes treatment of the direct effect of aerosols and the first and second indirect effects of aerosols on warm clouds (Kirkevåg et al., 2013). The atmospheric model is coupled to the Miami Isopycnic Coordinate Ocean Model (MICOM), which has a horizontal resolution of ~1.125° along the equator and 53 vertical levels. A detailed description of the model used in this study can be found in Bentsen et al. (2013) and Iversen et al. (2013). NorESM is among the best performing coupled climate models in representing ENSO relative to the mean climate state of the tropical Pacific and the spectrum of ENSO variability (Bellenger et al., 2014). In NorESM, the ENSO compares favorably to observations (see Figure 13 in Bellenger et al. (2014)) both in terms of mean state (amplitude, spatial structure, frequency spectrum, and the seasonality) and the strength of the feedbacks acting throughout a typical ENSO cycle (the Bjerknes feedback, the heat flux, shortwave and latent heat feedbacks). While NorESM still shows a climatological double-ITCZ in the Pacific Ocean, the bias is smaller relative to other climate models (Bentsen et al., 2013; Pausata, Grini, et al., 2015).

2.2. Experimental Design

We performed a series of experiments of 40 ensemble simulations each starting from two specific instants in time selected from a historical transient run forced by anthropogenic greenhouse gas and aerosol forcing from 1850—

2005. These two initial conditions from the transient simulation are used in both our aerosol forcing experiments ("volcano") and in the reference volcanically-unperturbed experiments ("no-volcano", NV) where the volcanic aerosol concentration is set to background conditions: 1 June 1923 and 1 June 1927. We chose 1 June 1923 as our starting date because the tropical Pacific is in an ENSO neutral state (Niño3.4 index = −0.1°C in June), but in the absence of an eruption is trending to La Niña conditions 3 months later (Niño3.4 index = −0.4°C in September; see Figure 2A in Pausata et al. (2020)). Unlike for 1 June 1923, the 1 June 1927 volcanic forcing is imposed upon a warm ENSO state (Niño3.4 index = +0.4°C) that, if not perturbed, remains warm for the next 18 months (see Figure 2a in Pausata et al. (2020)). The two different initial ENSO states allow to account for uncertainty in the ENSO response due to ocean preconditioning (Pausata, Karamperidou, et al., 2016; Predybaylo et al., 2020). For each of the two initial conditions, 20 simulations are performed with slightly modified initial conditions. The difference between the ensemble mean climate state induced by prescribing volcano aerosol forcing (MC, EqPAC or NAFR) and the unperturbed climate state (NV) shows the time history of the response to that forcing in terms of paired anomalies (Pausata, Grini, et al., 2015; Zanchettin et al., 2022) and illuminates the impact of forcing on the evolution of ENSO. For example, the change in surface temperature (TS) due to forcing over the MC, net of the natural evolution of the unperturbed climate system, is $\Delta TS_{MC} = T_{MC} - T_{NV}$. Figures in the paper show the average response over all 40 ensemble members.

The volcano experiments are highly idealized experiments in which a prescribed aerosol forcing is imposed in different areas of the tropics through prescribed changes in the aerosol mass mixing ratio. The imposed aerosol mass mixing ratio corresponds to an aerosol optical depth (AOD) anomaly peaking in August/September at about 0.4/0.5 at 550 nm either over the EqPAC, the MC or tropical and northern Africa (NAFR). The resulting radiative forcing peaks in the first summer when the forcing is applied and it amounts to about −8 W/m^2 in the region where the volcanic aerosol forcing is applied (Figure S1 in Supporting Information S1); and the forcing fades away returning to background AOD values after 1.5 years. The imposed AOD anomaly corresponds to the zonal mean AOD anomaly estimated in the tropical regions following a Tambora eruption (Zanchettin, Khodri, et al., 2016). As we imposed the aerosol mass mixing ratio anomalies over specific areas, there is no transport of volcanic aerosols outside the forcing region. We perform two additional experiments in which extreme AOD anomalies (∼3 times larger than in the previous case) are applied over the Maritime Continent (MCext) and the Equatorial Pacific (EqPACext) to account for the fact that many tropical eruptions occur in the MC, where much higher aerosol concentrations than the zonal average typically develop, particularly in the first post-eruption months (Figure S2 in Supporting Information S1). The maximum radiative forcing of about −22 W/m^2 peaks in the first September following the aerosol perturbation (Figure S1 in Supporting Information S1). The prescribed SO$_4$ gradient at the borders of the forcing regions where the aerosol forcing is imposed is not dissimilar from the gradients that develop in experiments where the volcanic plume is allowed to evolve (see e.g., Figures 2a and 2b, in the TrNH eruptions in Pausata et al. (2020)). Therefore, it does not, in itself, present an additional or unique unrealistic forcing that could unduly affect the results.
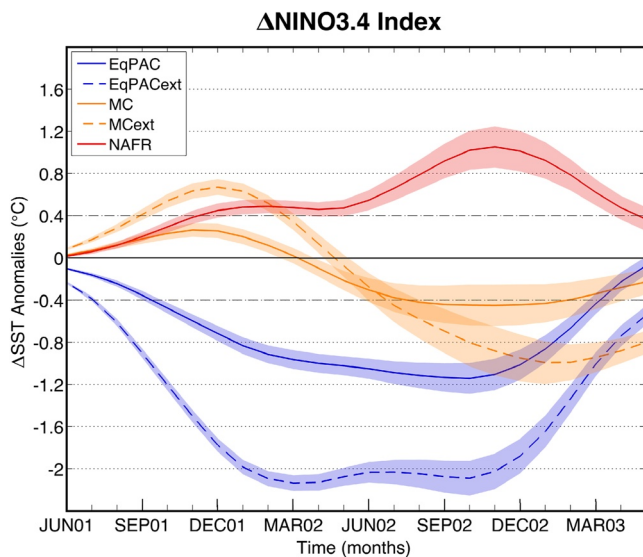
In the MC experiments, we prescribe an increased SO$_4$ mixing ratio over the region between 10°S and 10°N and 100°E to 150°E, and we extend it to cover 100°E to 80°W in the EqPAC experiment. In the NAFR experiments the imposed aerosol forcing extends from 10°S to 33°N and from 20°W to 55°E. We opted for prescribing the aerosol forcing over the specific area of interest rather than simulating interactively a volcanic eruption to test the above-mentioned mechanisms. This experimental design precludes extratropical forcing and hemispheric asymmetry in forcing that would accompany any tropical eruption by way of the Brewer-Dobson circulation (Toohey et al., 2011) and, thus, isolates the impact of tropical aerosol forcing.

To evaluate whether spurious responses may be triggered by a sharp spatial discontinuity in the applied forcing, we performed an additional experiment (EqPACsmooth) in which the volcanic aerosol anomalies of the EqPAC simulations are tapered to 75%, 50%, 25%, 10%, and 5% of the max forcing over a distance of ∼1,000 km (5 grid boxes) (Figure S2 in Supporting Information S1). The climate response to the smoothed forcing is very similar to the case when no smoothing is applied (Figures S3 and S4 in Supporting Information S1). The temperature and precipitation anomalies are slightly larger in the smoothed forcing experiment because the forcing is overall stronger due to the extended area over which the aerosol spread out. Furthermore, anomalies in the stratospheric circulation are not sensitive to the sharpness of the forcing, building confidence on the fact that spurious stratospheric dynamics do not affect the tropospheric response which is the focus of this study (see Figure S5 in Supporting Information S1 for further details). This sensitivity test confirms the robustness of the approach used in our work.
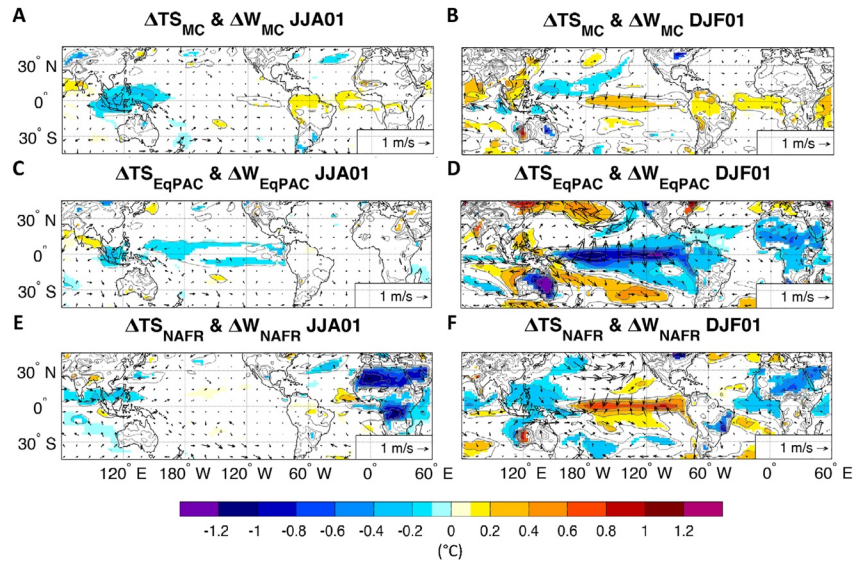
Figure 2. Surface temperature and wind response. Changes in surface temperature (°C, contours and shadings) and wind (m/s, arrows) in the summer (June to August—JJA; left) and winter (December to February—DJF; right) following the aerosol optical depth imposed anomalies above the Maritime Continent (MC) (a) and (b), the equatorial Pacific (EqPAC) (c) and (d), and the tropical and northern Africa—NAFR (e) and (f) relative to the no-volcano experiment. Only temperature values that are significantly different at the 5% level using a local (grid-point) t test are shaded. The contours follow the colorbar intervals (solid for positive and dashed for negative anomalies; the zero line is omitted).

The ENSO index used in this study is based on monthly SST anomalies averaged over the Niño3.4 region (5°N–5°S; 170°W–120°W). We apply a 5-month running mean to remove intraseasonal variations in SST. An El Niño event is defined when the Niño3.4 index exceeds 1 SD (+0.4°C) for at least six consecutive months. Unless otherwise noted, all differences discussed in this study are significant at the 95% confidence level using a Student's t test.
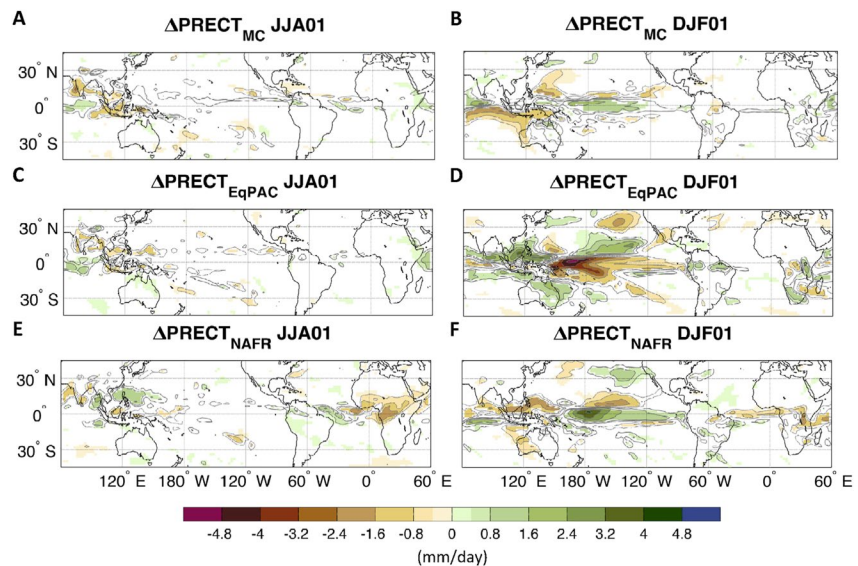
In our study we analyze the SST rather than relative SST as recommended when investigating the ENSO response to volcanic eruptions to isolate the dynamical ENSO signal from the tropical radiative surface cooling. In our case the aerosol forcing is confined to a small portion of the tropical belt; consequently, possible interferences by circumglobal tropical cooling are not present. Therefore, the use of raw SST is justified in our study.

3. Results

3.1. The MC Cooling and ODT Mechanisms

When a uniform stratospheric volcanic aerosol loading is applied over the MC (experiment) a cooling is simulated over the entire region in the following months (Figure 2a). The MC cooling triggers weak westerly wind anomalies (Figure 2a and Figure S6a in Supporting Information S1) as an area of low-level divergence develops over the MC (Figure S6a in Supporting Information S1). These changes then give rise to a modest El Niño-like response in the first perturbed winter (Figure 2b). The warm anomalies fade away by the end of the spring and La Niña-like conditions start developing in the second perturbed summer (Figure 3 and Figure S7B in Supporting Information S1).

When the aerosol loading is extended to the entire EqPAC experiment, the surface response in the EqPAC is a weak cooling during the first 3 months when the volcanic aerosol anomalies are imposed (Figures 2c and 3). The cooling extends from the western seaboard of South America to the MC

Figure 3. Simulated El Niño-Southern Oscillation response. Changes in the Niño3.4 index for each ensemble experiment relative to the no-volcano case. Shading represents twice the standard error of the mean (approximate 95% confidence intervals).

Figure 4. Rainfall response. Changes in precipitation (mm/day, contours and shadings) in the first summer (June to August—JJA; left) and winter (December to February—DJF; right) following the AOD imposed anomalies above the Maritime Continent—MC (a) and (b), the equatorial Pacific—EqPAC (c) and (d) and the tropical and northern Africa—NAFR (e) and (f) relative to the no-volcano experiment. Only precipitation values that are significantly different at the 5% level using a local (grid-point) *t* test are shaded. The contours follow the colorbar intervals (solid for positive and dashed for negative anomalies; the zero line is omitted).

(Figure 2c) and is accompanied by a weak intensification of the trade winds (Figure 2c and Figure S6c in Supporting Information S1). The intensification of the trade winds over the central and western tropical Pacific seems to be related to an anomalous zone of convergence that develops in the western Indian Ocean (Figure 4c and Figure S6c in Supporting Information S1). These results are opposite to what would occur if the ODT mechanism were the dominant reason for the changes in the evolution of ENSO after a tropical eruption. The easterly wind anomalies intensify in the following months and La Niña-like conditions develop in the first post-eruption winter (Figure 2d and Figure S8c in Supporting Information S1). The cooling is not restricted to the surface and therefore a simple direct response to the radiative forcing, but it extends deeper till the thermocline, showing the classical La Niña pattern (Figure S8c in Supporting Information S1). The cold anomalies over the EqPAC persist into the following year peaking in the second fall after the perturbation is applied (Figure 2 and Figure S8d in Supporting Information S1).

The temperature and precipitation anomalies after the aerosol perturbation are not confined to the area where the forcing is applied but spread across the world following—to a large extent—the classical ENSO teleconnections (Figures 2 and 4). In the MC experiment the global anomalies are weak and resemble those associated with an El Niño event, with wetting over the central western Pacific, and drying over the western MC, northern and western Australia, and northern Brazil (Figures 4a and 4b). In the EqPAC experiment, where a La Niña-like response takes place in the boreal winter, the anomalies are mostly of opposite sign compared to the MC experiment. The ITCZ also shifts northward in the Pacific Ocean (Figures 4c and 4d).

Repeating the MC and EqPAC experiments but with extreme aerosol loading (called MCext and EqPACext, respectively) shows similar spatial patterns of SST and precipitation anomalies but with larger amplitude (cf. Figures 2 and 4 to Figures S9 and S10 in Supporting Information S1): a moderate El Niño-like response for the MCext experiment and a very intense La Nina-like response (with cooling exceeding 2°C) developing in the EqPACext ensemble (Figure 3 and Figure S9 in Supporting Information S1).

3.2. The Tropical and Northern African Cooling

In the NAFR experiment the aerosol loading is confined from NAFR to 10°S (Figures 1e and 1f). The AOD anomalies cause a cooling of up to 1–1.2°C over the Sahara region and south of the equator (Figure 2e). The cooling causes a drying of about 1–2 mm/day in the sub-Saharan regions (Figure 4e). The reduction in rainfall

and the cooling around the equatorial regions in Africa cause a Matsuno–Gill response (Gill, 1980) that alters the Walker Circulation (Figure S6e in Supporting Information S1) and induces easterly wind anomalies over the Atlantic and westerly wind anomalies over the equatorial Indian and western Pacific Oceans (Figure 2e and Figure S6e in Supporting Information S1). The shift in the Walker circulation leads to a reduced convection over the western Pacific that further strengthens the westerly wind signal (Figure 2f and Figure S6f in Supporting Information S1). In the equatorial Atlantic, an Atlantic Niña-like develops due to the easterly wind anomalies shallowing the thermocline. The westerly wind anomaly in the western EqPAC triggers oceanic downwelling Kelvin waves that travel eastward reaching the eastern Pacific in the winter following the applied forcing (Figure S8e in Supporting Information S1). The anomalous Kelvin waves deepen the thermocline in the central and eastern Pacific (Figure S8e in Supporting Information S1) contributing to the development of an El Niño. During the summer of the following year, the cooling and drying over tropical NAFR is no longer present. However, persistence of the Atlantic La Niña-like anomaly (Figure S11e in Supporting Information S1) contributes to enhancing westerly wind anomalies over the Pacific (Figure S8e in Supporting Information S1), favoring the continuation of El Niño-like conditions as pointed out in recent studies (Li et al., 2016; Rodríguez-Fonseca et al., 2009; Pausata et al., 2017; Zanchettin, Bothe, et al., 2016).

The results from the NAFR experiment are in broad agreement with the study of Khodri et al. (2017), who also found that the cooling and drying of tropical Africa initiate westerly wind anomalies over western Pacific oceans able to affect ENSO for two consecutive years, and additionally point to a possible westward pathway for the northern African mechanism through the Atlantic Niña phenomenon.

4. Discussion and Conclusions

This study provides the first attempt to explore different mechanisms governing the ENSO response to stratospheric aerosol forcing through idealized coupled climate model experiments where the aerosol enhancement is confined regionally. The rationale is that regionally confined aerosol loading initiates regionally confined surface cooling. Three mechanisms can be tested by our approach, all operating through radiatively forced changes in surface temperature and potentially relevant for volcanically-forced climate variability, namely the "ODT"; (b) the cooling of the MC; and (c) the cooling of tropical NAFR mechanism. Among the three mechanisms investigated here, our results point to the tropical NAFR and the MC as the regions over which the cooling induced by aerosol forcing increases the likelihood of El Niño events. The MC cooling mechanism may in principle be able to explain the tendency for positive ENSO phases following volcanic eruptions: El Niño-like anomalies are indeed simulated following a differential cooling between the MC and the central-western Pacific Ocean following the aerosol perturbation (Figure 2a). The MC mechanism requires stronger forcing than the NAFR mechanism to be detected (see the MCext experiment) and it relies on the land cooling faster than the ocean. However, when the aerosol forcing is extended to the nearby EqPAC as in the EqPAC (Figure 1c), the MC does not cool more than the ocean, whereas a uniform cooling spreads from the western to the eastern side of the basin (Figure 2a and Figure S8 in Supporting Information S1) and La Niña-like anomalies subsequently develop. Therefore, the MC cooling mechanism does not work when the volcanic aerosol extends well into the EqPAC, which is usually the case following tropical volcanic eruptions (Zanchettin, Bothe, et al., 2016). Furthermore, our EqPAC experiment also highlights that the preferential cooling of the western Pacific ocean relative to the eastern EqPAC, the signature of the ODT mechanism that would give rise to El Niño-like anomalies, does not occur. One possible explanation is that uniform aerosol forcing over the tropical Pacific causes important anomalies in convection over the Indian Ocean that enhance the trade winds in the Pacific, triggering La Niña-like anomalies. However, the Indian Ocean response was not included in the ODT mechanism. Another reason could be related to the fact that in the studies using the Zebiak-Cane model (Clement et al., 1996; Emile-Geay et al., 2008; Mann et al., 2005) the uniform forcing (cooling) is imposed at the ocean surface, whereas in our case we impose a uniform forcing in the stratosphere. Because of the more extensive climatological cloud cover in the equatorial western compared to eastern Pacific (Figure S12 in Supporting Information S1), the forcing at the ocean surface associated with a volcanic eruption will be weaker there than in the eastern Pacific, which would act to counteract the ODT mechanism and give rise to a more uniform SST cooling.

Based on current understanding, the development of an El Niño response following volcanic eruptions is likely associated with eruptions in which the aerosol loading is either spread rather uniformly across the hemispheres or is mostly confined to the Northern Hemisphere (NH). Such aerosol distributions allow a cooling of NAFR as well

as a larger cooling of the NH relative to the Southern Hemisphere, which will also trigger a southward displacement of the ITCZ (Pausata, Chafik, et al., 2015, 2020; Ward et al., 2021). Both mechanisms—NAFR cooling and southward ITCZ shift—will constructively superpose to trigger a weakening of the trades along the EqPAC and therefore lead to El Niño-like anomalies. Pausata et al. (2020) also suggest a potential role of the extratropics in which the extratropical response to volcanic aerosol radiative forcing mediates the ENSO response favoring El Niño-like anomalies. Our sensitivity experiments allow to evaluate individually mechanisms of ENSO response to volcanic forcing; however, in the real world the ENSO response is a combination—non necessary linear—of all such mechanisms, whose individual relative role may also be significantly affected by background climate conditions. Furthermore, our results refer only to one model and may therefore be affected by its biases, including those regarding ENSO and the ITCZ. For example, Seager et al. (2019) argue that the cold tongue bias in climate models results in an El Nino-like response to increasing greenhouse gas concentrations. Therefore, if the relation were linear, a global cooling should be associated with La Nina-like conditions. However, our model does not seem to be affected by such bias, as it does not show any changes in the temperature gradient in the Pacific with increasing GHGs (see Figure 4e in Iversen et al. (2013)). Furthermore, our model also displays the opposite response (El Niño-like) when global cooling is forced, for example, by a nuclear explosion (Pausata, Lindvall, et al., 2016) or a volcanic eruption (Pausata et al., 2020) an El Niño-like response is simulated.

Our study provides clues for the design of coordinated multi-model experiments to individually evaluate mechanisms contributing to the climate response to volcanic eruptions and their different representation in different numerical models. Currently, the Model Intercomparison Project on the climatic response to Volcanic forcing (VolMIP, (Zanchettin, Khodri, et al., 2016)) tackles questions related to the spatial structure of the forcing only by considering idealized eruptions where the volcanic aerosol is confined either in the northern or the southern hemisphere. Whereas these experiments can shed light on the role of the ITCZ mechanism (Pausata et al., 2020), a set of easy-to-implement idealized forcing experiments with regionally-confined aerosol as the one proposed here would allow to evaluate the robustness across models of regional mechanisms contributing to the ENSO response to volcanic forcing. Ultimately, this will increase confidence about the predictability of ENSO during periods of strong volcanism.

Conflict of Interest

The authors declare no conflicts of interest relevant to this study.

Data Availability Statement

The datasets generated and analyzed in this study is archived in https://figshare.com/s/2468a3c81dbcb30032ce (https://doi.org/10.6084/m9.figshare.20349090).

References

Adams, J. B., Mann, M. E., & Ammann, C. M. (2003). Proxy evidence for an El Niño-like response to volcanic forcing. *Nature*, *426*(6964), 274–278. https://doi.org/10.1038/nature02101

Atwood, A. R., Donohoe, A., Battisti, D. S., Liu, X., & Pausata, F. S. R. (2020). Robust longitudinally variable responses of the ITCZ to a myriad of climate forcings. *Geophysical Research Letters*, *47*(17), e2020GL088833. https://doi.org/10.1029/2020GL088833

Bellenger, H., Guilyardi, E., Leloup, J., Lengaigne, M., & Vialard, J. (2014). ENSO representation in climate models: From CMIP3 to CMIP5. *Climate Dynamics*, *42*(7–8), 1999–2018. https://doi.org/10.1007/s00382-013-1783-z

Bentsen, M., Bethke, I., Debernard, J. B., Iversen, T., Kirkevag, A., Seland, O., et al. (2013). The Norwegian Earth System Model, NorESM1-M—Part 1: Description and basic evaluation of the physical climate. *Geoscientific Model Development*, 6(3), 687–720. https://doi.org/10.5194/gmd-6-687-2013

Bjerknes, J. (1969). Atmospheric teleconnections from the equatorial Pacific. *Monthly Weather Review*, *97*(3), 163–172. https://doi.org/10.1175/1520-0493(1969)097<0163:ATFTEP>2.3.CO;2

Christiansen, B. (2008). Volcanic eruptions, large-scale modes in the northern hemisphere, and the El Niño–southern oscillation. *Journal of Climate*, *21*(5), 910–922. https://doi.org/10.1175/2007JCLI1657.1

Clement, A. C., Seager, R., Cane, M. A., & Zebiak, S. E. (1996). An ocean dynamical thermostat. *Journal of Climate*, 9(9), 2190–2196. https://doi.org/10.1175/1520-0442(1996)009<2190:AODT>2.0.CO;2

Colose, C. M., LeGrande, A. N., & Vuille, M. (2016). Hemispherically asymmetric volcanic forcing of tropical hydroclimate during the last millennium. *Earth System Dynamics*, *7*(3), 681–696. https://doi.org/10.5194/esd-7-681-2016

Dee, S. G., Cobb, K. M., Emile-Geay, J., Ault, T. R., Edwards, R. L., Cheng, H., & Charles, C. D. (2020). No consistent ENSO response to volcanic forcing over the last millennium. *Science*, *367*(6485), 1477–1481. https://doi.org/10.1126/science.aax2000

Emile-Geay, J., Seager, R., Cane, M. A., Cook, E. R., & Haug, G. H. (2008). Volcanoes and ENSO over the past millennium. *Journal of Climate*, *21*(13), 3134–3148. https://doi.org/10.1175/2007JCLI1884.1

Gill, A. E. (1980). Some simple solutions for heat-induced tropical circulation. *Quarterly Journal of the Royal Meteorological Society*, *106*(449), 447–462. https://doi.org/10.1002/qj.49710644905

Hirono, M. (1988). On the trigger of El Niño southern oscillation by the forcing of early El Chichón volcanic aerosols. *Journal of Geophysical Research*, *93*(D5), 5365. https://doi.org/10.1029/JD093iD05p05365

Iversen, T., Bentsen, M., Bethke, I., Debernard, J. B., Kirkevag, A., Seland, O., et al. (2013). The Norwegian Earth system model, NorESM1-M—Part 2: Climate response and scenario projections. *Geoscientific Model Development*, *6*(2), 389–415. https://doi.org/10.5194/gmd-6-389-2013

Kang, S. M., Held, I. M., Frierson, D. M. W., & Zhao, M. (2008). The response of the ITCZ to extratropical thermal forcing: Idealized slab-ocean experiments with a GCM. *Journal of Climate*, *21*(14), 3521–3532. https://doi.org/10.1175/2007JCLI2146.1

Khodri, M., Izumo, T., Vialard, J., Janicot, S., Cassou, C., Lengaigne, M., et al. (2017). Tropical explosive volcanic eruptions can trigger El Niño by cooling tropical Africa. *Nature Communications*, *8*(1), 778. https://doi.org/10.1038/s41467-017-00755-6

Kirkevåg, A., Iversen, T., Seland, O., Hoose, C., Kristjansson, J. E., Struthers, H., et al. (2013). Aerosol-climate interactions in the Norwegian Earth system model—NorESM1-M. *Geoscientific Model Development*, *6*(1), 207–244. https://doi.org/10.5194/gmd-6-207-2013

Kodera, K. (1994). Influence of volcanic eruptions on the troposphere through stratospheric dynamical processes in the northern hemisphere winter. *Journal of Geophysical Research*, *99*(D1), 1273. https://doi.org/10.1029/93JD02731

Li, J., Xie, S. P., Cook, E. R., Morales, M. S., Christie, D. A., Johnson, N. C., et al. (2013). El Niño modulations over the past seven centuries. *Nature Climate Change*, *3*(9), 822–826. https://doi.org/10.1038/nclimate1936

Li, X., Xie, S.-P., Gille, S. T., & Yoo, C. (2016). Atlantic-induced pan-tropical climate change over the past three decades. *Nature Climate Change*, *6*(3), 275–279. https://doi.org/10.1038/nclimate2840

Mann, M. E., Cane, M. A., Zebiak, S. E., & Clement, A. (2005). Volcanic and solar forcing of the tropical Pacific over the past 1000 years. *Journal of Climate*, *18*(3), 447–456. https://doi.org/10.1175/JCLI-3276.1

McGregor, S., Khodri, M., Maher, N., Ohba, M., Pausata, F. S. R., & Stevenson, S. (2020). The effect of strong volcanic eruptions on ENSO. In *El Niño southern oscillation in a changing climate* (pp. 267–287). Geophysical Monograph Series, American Geophysical Union.

McGregor, S., & Timmermann, A. (2011). The effect of explosive tropical volcanism on ENSO. *Journal of Climate*, *24*(8), 2178–2191. https://doi.org/10.1175/2010JCLI3990.1

Neale, R. B., Richter, J., Park, S., Lauritzen, P. H., Vavrus, S. J., Rasch, P. J., & Zhang, M. (2013). The mean climate of the Community atmosphere model (CAM4) in forced SST and fully coupled experiments. *Journal of Climate*, *26*(14), 5150–5168. https://doi.org/10.1175/JCLI-D-12-00236.1

Ohba, M., Shiogama, H., Yokohata, T., & Watanabe, M. (2013). Impact of strong tropical volcanic eruptions on ENSO simulated in a coupled GCM. *Journal of Climate*, *26*(14), 5169–5182. https://doi.org/10.1175/jcli-d-12-00471.1

Pausata, F. S. R., Chafik, L., Caballero, R., & Battisti, D. S. (2015). Impacts of high-latitude volcanic eruptions on ENSO and AMOC. *Proceedings of the National Academy of Sciences*, *112*(45), 13784–13788. https://doi.org/10.1073/pnas.1509153112

Pausata, F. S. R., Grini, A., Caballero, R., Hannachi, A., & Seland, Ø. (2015). High-latitude volcanic eruptions in the Norwegian Earth System Model: The effect of different initial conditions and of the ensemble size. *Tellus Series B Chemical and Physical Meteorology*, *67*(26728), 26728. https://doi.org/10.3402/tellusb.v67.26728

Pausata, F. S. R., Karamperidou, C., Caballero, R., & Battisti, D. S. (2016). ENSO response to high-latitude volcanic eruptions in the Northern Hemisphere: The role of the initial conditions. *Geophysical Research Letters*, *43*(16), 8694–8702. https://doi.org/10.1002/2016GL069575

Pausata, F. S. R., Lindvall, J., Ekman, A. M. L., & Svensson, G. (2016). Climate effects of a hypothetical regional nuclear war: Sensitivity to emission duration and particle composition. *Earth's Future*, *4*(11), 498–511. https://doi.org/10.1002/2016EF000415

Pausata, F. S. R., Zanchettin, D., Karamperidou, C., Caballero, R., & Battisti, D. S. (2020). ITCZ shift and extratropical teleconnections drive ENSO response to volcanic eruptions. *Science Advances*, *6*(23), eaaz5006. https://doi.org/10.1126/sciadv.aaz5006

Pausata, F. S. R., Zhang, Q., Muschitiello, F., Lu, Z., Chafik, L., Niedermeyer, E. M., et al. (2017). Greening of the Sahara suppressed ENSO activity during the mid-Holocene. *Nature Communications*, *8*(1), 16020. https://doi.org/10.1038/ncomms16020

Predybaylo, E., Stenchikov, G., Wittenberg, A. T., & Osipov, S. (2020). El Niño/Southern Oscillation response to low-latitude volcanic eruptions depends on ocean pre-conditions and eruption timing. *Commun. Earth Environ.*, *1*(1), 12. https://doi.org/10.1038/s43247-020-0013-y

Predybaylo, E., Stenchikov, G. L., Wittenberg, A. T., & Zeng, F. (2017). Impacts of a Pinatubo-size volcanic eruption on ENSO. *Journal of Geophysical Research: Atmospheres*, *122*(2), 925–947. https://doi.org/10.1002/2016JD025796

Rodríguez-Fonseca, B., Polo, I., García-Serrano, J., Losada, T., Mohino, E., Mechoso, C. R., & Kucharski, F. (2009). Are Atlantic Niños enhancing Pacific ENSO events in recent decades? *Geophysical Research Letters*, *36*(20), L20705. https://doi.org/10.1029/2009GL040048

Schneider, T., Bischoff, T., & Haug, G. H. (2014). Migrations and dynamics of the intertropical convergence zone. *Nature*, *513*(7516), 45–53. https://doi.org/10.1038/nature13636

Seager, R., Cane, M., Henderson, N., Lee, D.-E., Abernathey, R., & Zhang, H. (2019). Strengthening tropical Pacific zonal sea surface temperature gradient consistent with rising greenhouse gases. *Nature Climate Change*, *9*(7), 517–522. https://doi.org/10.1038/s41558-019-0505-x

Shindell, D. T. (2004). Dynamic winter climate response to large tropical volcanic eruptions since 1600. *Journal of Geophysical Research*, *109*(D5), D05104. https://doi.org/10.1029/2003JD004151

Stevenson, S., Otto-Bliesner, B., Fasullo, J., & Brady, E. (2016). "El Niño like" hydroclimate responses to last millennium volcanic eruptions. *Journal of Climate*, *29*(8), 2907–2921. https://doi.org/10.1175/JCLI-D-15-0239.1

Thompson, D. W. J., Wallace, J. M., Jones, P. D., & Kennedy, J. J. (2009). Identifying signatures of natural climate variability in time series of global-mean surface temperature: Methodology and insights. *Journal of Climate*, *22*(22), 6120–6141. https://doi.org/10.1175/2009JCLI3089.1

Timmreck, C. (2012). Modeling the climatic effects of large explosive volcanic eruptions. *Wiley Interdiscip. Rev. Clim. Chang.*, *3*(6), 545–564. https://doi.org/10.1002/wcc.192

Toohey, M., Krüger, K., Niemeier, U., & Timmreck, C. (2011). The influence of eruption season on the global aerosol evolution and radiative impact of tropical volcanic eruptions. *Atmospheric Chemistry and Physics*, *11*(23), 12351–12367. https://doi.org/10.5194/acp-11-12351-2011

Ward, B., Pausata, F. S. R., & Maher, N. (2021). The sensitivity of the El Ninō-Southern Oscillation to volcanic aerosol spatial distribution in the MPI Grand Ensemble. *Earth Syst. Dyn.*, *12*(3), 975–996. https://doi.org/10.5194/esd-12-975-2021

Zanchettin, D. (2017). Aerosol and solar irradiance effects on decadal climate variability and predictability. *Current Climate Change Reports*, *3*(2), 150–162. https://doi.org/10.1007/s40641-017-0065-y

Zanchettin, D., Bothe, O., Graf, H. F., Omrani, N., Rubino, A., & Jungclaus, J. H. (2016). A decadally delayed response of the tropical Pacific to Atlantic multidecadal variability. *Geophysical Research Letters*, *43*(2), 784–792. https://doi.org/10.1002/2015GL067284

Zanchettin, D., Khodri, M., Timmreck, C., Toohey, M., Schmidt, A., Gerber, E. P., et al. (2016). The Model Intercomparison Project on the climatic response to Volcanic forcing (VolMIP): Experimental design and forcing input data for CMIP6. *Geoscientific Model Development*, *9*(8), 2701–2719. https://doi.org/10.5194/gmd-9-2701-2016

Zanchettin, D., Timmreck, C., Khodri, M., Schmidt, A., Toohey, M., Abe, M., et al. (2022). Effects of forcing differences and initial conditions on inter-model agreement in the VolMIP volc-pinatubo-full experiment. *Geoscientific Model Development*, *15*(5), 2265–2292. https://doi.org/10.5194/gmd-15-2265-2022

Zebiak, S. E., & Cane, M. A. (1987). A model El Nino–southern oscillation. *Monthly Weather Review*, *115*(10), 2262–2278. https://doi.org/10.1175/1520-0493(1987)115<2262:AMENO>2.0.CO;2

Zuo, M., Man, W., Zhou, T., & Guo, Z. (2018). Different impacts of northern, tropical, and southern volcanic eruptions on the tropical Pacific SST in the last millennium. *Journal of Climate*, *31*(17), 6729–6744. https://doi.org/10.1175/JCLI-D-17-0571.1